

Title	A novel strictly NADPH-dependent <i>Pichia stipitis</i> xylose reductase constructed by site-directed mutagenesis.
Author(s)	Khattab, Sadat Mohammad Rezq; Watanabe, Seiya; Saimura, Masayuki; Kodaki, Tsutomu
Citation	Biochemical and biophysical research communications (2011), 404(2): 634-637
Issue Date	2011-01-14
URL	http://hdl.handle.net/2433/134797
Right	© 2010 Elsevier Inc.
Type	Journal Article
Textversion	author

1 **A Novel Strictly NADPH-Dependent *Pichia stipitis* Xylose Reductase Constructed by**
2 **Site-directed Mutagenesis**

3 **Sadat Mohammad Rezq Khattab^{1,2}, Seiya Watanabe¹, Masayuki Saimura¹,**
4 **Tsutomu Kodaki^{1*}**

5 ¹ Institute of Advanced Energy, Kyoto University, Gokasho, Uji, Kyoto 611-0011, Japan

6 ² Faculty of Science, Al-Azhar University, Assiut Branch 71524, Egypt

7
8 **Abstract**

9 Xylose reductase (XR) and xylitol dehydrogenase (XDH) are the key enzymes for
10 xylose fermentation and have been widely used for construction of a recombinant xylose
11 fermenting yeast. The effective recycling of cofactors between XR and XDH has been
12 thought to be important to achieve effective xylose fermentation. Efforts to alter the
13 coenzyme specificity of XR and HDX by site-directed mutagenesis have been widely
14 made for improvement of efficiency of xylose fermentation. We previously succeeded by
15 protein engineering to improve ethanol production by reversing XDH dependency from
16 NAD⁺ to NADP⁺. In this study, we applied protein engineering to construct a novel
17 strictly NADPH dependent XR from *Pichia stipitis* by site-directed mutagenesis, in order
18 to recycle NADPH between XR and XDH effectively. One double mutant, E223A/S271A
19 showing strict NADPH dependency with 106 % activity of wild-type was generated. A
20 second double mutant, E223D/S271A, showed a 1.27-fold increased activity compared to
21 the wild-type XR with NADPH and almost negligible activity with NADH.

22
23 *Keywords:* Coenzyme specificity, Xylose reductase, Site-directed mutagenesis

25 *Corresponding author. Mailing address: Institute of Advanced Energy, Kyoto University,
26 Gokasyo, Uji 611-0011, Japan Phone: 81-774-38-3510. Fax: 81-774-38-3524.
27 E-mail: kodaki@iae.kyoto-u.ac.jp

28

29 **1. Introduction**

30 Xylose is the second most abundant pentose sugar constituting the lignocellulosic
31 renewable biomass after glucose, and its complete fermentation is economically valuable
32 for producing biofuel from lignocellulosic biomass [6]. Recombinant *S. cerevisiae* can
33 ferment xylose through a fungal pathway involving two heterologous oxidoreductase
34 genes. In this pathway, *Pichia stipitis* xylose reductase (PsXR) (XR; EC 1.1.1.21) [18],
35 which prefers NADPH, reduces xylose to xylitol followed by *P. stipitis* xylitol
36 dehydrogenase (PsXDH), which exclusively requires NAD⁺ (XDH; EC 1.1.1.9) [17],
37 oxidizes xylitol into xylulose. *S. cerevisiae* xylulokinase (XK) (EC 2.7.1.17) naturally
38 phosphorylates xylulose to xylulose-5-phosphate, which is then metabolized by the
39 glycolytic pathway via the pentose phosphate pathway [7]. XK overexpression improves
40 the efficiency of xylose fermentation [4, 5, 15]. Although this fungal pathway is highly
41 expressed in *S. cerevisiae*, the efficiency of ethanol production is somewhat obstructed by
42 the unfavorable accumulation of xylitol due to the imbalance of coenzyme specificities
43 between XR and XDH [6].

44 Xylose reductase is a member of the aldo-keto reductase (AKR) superfamily
45 which is made up of 14 different families and approximately 120 members with a
46 majority of dual cofactor type enzymes [8]. *Candida tenuis* XR (CtXR) is one of these
47 enzymes. Its crystal structure has been determined at different levels of resolution and its
48 binding sites with NAD(P)H were also determined [10,12, 25]. Although only little

49 structural information of PsXR is available, it has about 76% homology with the CtXR.
50 This high percentage of similarity should provide some clues for manipulation of PsXR
51 [13].

52 Protein engineering has been widely used to alter the coenzyme specificity of XR
53 and XDH. Since PsXDH accepts only NAD⁺, many researchers reversed the preference
54 of XR to NADH in order to achieve NAD⁺/NADH cofactor recycling [1, 13, 16, 20]. On
55 the other hand, we have been working on converting cofactor usage of XDH to NADP⁺
56 from NAD⁺ [21]. We previously succeeded to improve the fermentation process and
57 ethanol production by using these XDH mutants [23]. In this study, site-directed
58 mutagenesis of PsXR was performed to construct a strictly NADPH-dependent XR,
59 expecting decreasing or preventing xylitol accumulation and subsequently improving
60 ethanol production.

61

62 **2. Materials and Methods**

63 2.1 Cloning of the *P. stipitis* Xylose reductase gene and Site-directed mutagenesis

64 A plasmid, named pHis (WT) harboring the His-tagged wild-type (WT) PsXR
65 gene was constructed as described previously [20]. All XR mutations were introduced by
66 site-directed mutagenesis, using the single round PCR method with *PfuTurbo* DNA
67 polymerase (Stratagene) and the PCR Thermal Cycler PERSONAL (TaKaRa, Otsu,
68 Japan). The codons used for mutations introduced in this study were as follows: E223A
69 (GAA→GCA), E223D (GAA→GAC), and S271A (TCC→GCC). The PCR products
70 were subjected to DpnI restriction enzyme treatment in order to digest the parent DNA
71 strands to prevent transformation of the template plasmid. Only nicked circular
72 mutagenic strands were transformed into *Escherichia coli* DH5a. Electroporation method

73 was used to transform plasmids and the mutations were confirmed by DNA sequencing
74 using Applied Biosystems 3031 genetic analyzer and ABI Prism[®] Big Dye[®] Terminator
75 v3.1 Cycle Sequencing kit.

76

77 2.2 Overexpression and purification of (His)₆-tagged enzymes

78 *P. stipitis* xylose reductase wild-type and mutated genes were expressed in *E. coli*
79 DH5 α and purified as described previously [20]. Purified enzymes were confirmed on
80 10 % acrylamide SDS-PAGE. Protein concentrations were determined using the Bio
81 RAD Quick Start Bradford 1x Dye Reagent (Bio-Rad Laboratories, CA, USA) by
82 measuring the absorbance at 595 nm with γ -globin as a standard.

83

84 2.3 Enzyme assays and Kinetic parameters

85 Enzyme activities were measured spectrophotometrically as described previously
86 [20] with modification in xylose concentration to 400 mM. The kinetic parameters were
87 calculated by Line Weaver–Burk plots.

88

89 **3. Result and Discussion**

90 3.1 Speculation and prediction of NAD(P)H binding sites

91 Crystallographic analyses of many AKRs have revealed that they share a common
92 (α/β)₈ barrel fold, with a highly conserved coenzyme binding pocket at the C-terminus.
93 90.9 % of the residues are located in the core area and 9.1 % are in the allowed regions
94 [11]. The nicotinamide ring of NAD(P)H is resides in the core of the barrel. Residues
95 Glu²²⁷ and Asn²⁷⁶ in CtXR, which equal to Glu²²³ and Asn²⁷² in PsXR, primarily mediate
96 the interactions with the adenosine ribose 2'- and 3'-hydroxy groups. As shown in Fig. 1,

97 Glu²²³ represents the essential part NADH binding where contacts by bidentate hydrogen
98 bond with both of the hydroxy groups. Similar interactions have been seen in many other
99 NADH-binding protein structures [2, 3]. However, The structurally equivalent residues
100 Asp²¹⁶ and Val²⁶⁴ in aldose reductase in human (AR) are unable to fulfill the equivalent
101 roles, Asp²¹⁶ is required for high affinity binding of NADPH by forming two salt linkages
102 with Lys²¹ and Lys²⁶² and fastening the loop over the co-substrate [24].

103 Glu²²⁷ and Lys²⁷⁴ in CtXR makes water-mediated interactions each other and with
104 the 3'-hydroxy group in the case of NADP⁺-bound structures. In the absence of a
105 negatively charged phosphate, Glu²²⁷ side chain is able to rotate into a favourable
106 conformation to accept a 2.64 Å hydrogen bond contact with the 2'-hydroxy group and a
107 2.65 Å hydrogen bond with the 3'-hydroxy group when NAD⁺ is bound. The root mean
108 square deviations of the C α values between NAD⁺- and NADP⁺-bound models was
109 calculated in CtXR. The largest conformational change is seen in residues 274–280,
110 which corresponding to 270-276 in PsXR, and then residues 225–229, which
111 corresponding to 221-225 in PsXR, a short helical region that appears at the end of β 7.
112 The largest main-chain shift is seen in Ser²⁷⁵, which corresponding to Ser²⁷¹ in PsXR,
113 moves 2.0 Å in response to the miss contact of the phosphate group of NADPH [10].
114 Furthermore, Glu²²³ of PsXR was subjected to a mutation trial and the result revealed that
115 alteration of this site might further inhibit NADH binding [13]. In addition, from the 3D
116 structure model of PsXR, it was reported that Glu²²³ and Phe²³⁶ can form 3 and 2
117 hydrogen bonds with NAD⁺, respectively [19].

118 Considering the property as described above, the mutations were designed based
119 on sequence alignment of some strictly NADPH dependent analogous enzymes in the
120 AKR family, such as AR, as shown in table1, where glutamic acid 223 was substituted by

121 aspartic acid. Both glutamic and aspartic acid are acidic side chain and fully ionized at
122 neutral pH and able to engage in hydrogen bonds, which is a necessary component for a
123 high affinity xylose binding site [9]. Alanine is a nonpolar side chain that does not bind
124 or give off protons, or participate in hydrogen or ionic bonds. Alanine can be worked as
125 oily or lipid-like that promotes hydrophobic interactions. Accordingly, we apply aspartic
126 acid and alanine to mutation trials instead of PsXR glutamic acid 223.

127

128 3.2 Strictly NADPH dependency on Glu²²³ mutants

129 We applied Glu²²³ residue for mutation trails in order to delete NADH dependency.
130 Although this residue is also shared in NADPH binding, some reports reveal that it
131 contributes more to the affinity of NADH, where it plays a role in the binding site by
132 binding two hydrogen bonds with 2' and 3' hydroxy groups of the adenosine ribose. In
133 addition to changes in hydrogen-bonding of the adenosine, the ribose unmistakably
134 adopts the 3'-*endo* conformation rather than the 2'-*endo* conformation seen in the NADP⁺-
135 bound form [10]. The enzyme activities with NADH were calculated after introduction of
136 Glu²²³ residue mutations (Fig. 2). No activity was detected for E223A with NADH while
137 E223D showed only 17 % of the activity of WT. In addition, catalytic efficiency was
138 decreased to 3.7 % of WT. Their activities with NADPH showed 52 % and 44 % of WT,
139 respectively. The catalytic efficiencies of E223A and E223D were 26 % and 15 % of WT
140 respectively. Although, these ratios were low compared with WT, E223D showed 2.54
141 and 3.9 fold improvement in NADPH/NADH ratio and k_{cat}/K_m respectively. E223A is a
142 completely NADPH dependent mutant, probably due to the change of 3'-*endo* ribose
143 conformation and miss contact of bidentate hydrogen bonds which was conserved in
144 NAD⁺ binding sites in most members of dual cofactor in AKR family.

145

146 3.3 Improvement of enzyme activities with double mutants

147 We previously reported that the mutation of Lys²⁷⁰ and Arg²⁷⁶ in PsXR improve
148 NADH preference [20], while S271A increased the preference for NADPH [22]. The
149 second rounds of mutations were done based on this data. Accordingly, combination of
150 S271A with Glu²²³ mutants was expected to increase the activity of XR with NADPH. As
151 shown in Fig. 1, S271A mutant showed improved NADPH preference, where the
152 activities with NADPH and NADH were 125% and 85% compared to WT respectively.
153 These data encouraged us to perform further investigations by combining S271A and
154 Glu²²³ mutants. A combination of site-directed mutations of the residues Glu²²³ and
155 S271A produced unique and unprecedented results. The double mutants E223A/S271A
156 (AA) and E223D/S271A (DA) showed improvement in the activities with NADPH
157 compared to single Glu²²³ mutants. As shown in Fig. 2, the activity of the double mutant
158 AA with NADPH was 106% compared to WT. As shown in Table 2, the k_{cat} of WT and
159 AA were 622 and 657 min^{-1} , respectively; their K_{m} for xylose were 97.1 and 226 mM,
160 respectively; and their catalytic efficiencies were 38.6 and 32.4 $\mu\text{M}^{-1}/\text{min}^{-1}$, respectively.
161 On the other hand, the activity of DA showed 15 % WT with NADH (Fig. 1) in addition
162 to K_{m} was increased 12.8-fold and k_{cat} decreased 3-fold (Table 2). As shown in Fig. 2, the
163 activity of DA with NADPH was increased 1.27-fold compared to WT; k_{cat} also increased
164 1.18-fold compared to WT, while catalytic efficiency was decreased to 93 % of WT and
165 K_{m} increased 1.26-fold compared to WT (see table 2). Thus we succeeded to construct a
166 novel strictly NADPH-dependent PsXR by combining the mutation at Glu²²³ and Ser²⁷¹
167 residues.

168 We previously succeeded in improving xylose fermentation and ethanol production
169 by combining PsXR WT with the mutated PsXDH which accepts only NADP⁺ (i.e.,
170 quadruple ARSdR mutant) [23], and overexpression of XK [14, 15]. It may provide
171 further clues for understanding of importance of coenzyme specificities of XR and XDH
172 using the strictly NADPH-dependent PsXR of this study together with the strictly
173 NADP⁺-dependent PsXDH [21]. It could possibly give more efficient xylose
174 fermentation by an effective recycling of coenzymes of NADPH between XR and XDH.

175

176 **Acknowledgements**

177 This work was supported by the New Energy and Industrial Technology
178 Development Organization (NEDO), Japan. It was also supported by the Global Center of
179 Excellence (GCOE) program for the “Energy Science in the Age of Global Warming,” a
180 Grant-in-Aid for Scientific Research from the Ministry of Education, Science, Sports, and
181 Culture, Japan.

182

183 **References**

184 [1] O. Bengtsson, B. Hahn-Hagerdal, M.F. Gorwa-Grauslund, Xylose reductase from
185 *Pichia stipitis* with altered coenzyme preference improves ethanolic xylose
186 fermentation by recombinant *Saccharomyces cerevisiae*, *Biotechnol. Biofuels* 2
187 (2009) 9.

188

189 [2] O. Carugo, P. Argos, NADP-dependent enzymes. 1. Conserved stereochemistry of
190 cofactor binding, *Proteins Struct. Funct. and Genet.* 28 (1997) 10-28.

191

- 192 [3] O. Carugo, P. Argos, NADP-dependent enzymes. 2. Evolution of the mono- and
193 dinucleotide binding domains, *Proteins Struct. Funct. and Genet.* 28 (1997) 29-40.
194
- 195 [4] A. Eliasson, C. Christensson, C.F. Wahlbom, B. Hahn-Hagerdal, Anaerobic xylose
196 fermentation by recombinant *Saccharomyces cerevisiae* carrying XYL1, XYL2,
197 and XKS1 in mineral medium chemostat cultures, *Appl. Environ. Microbiol.* 66
198 (2000) 3381-3386.
199
- 200 [5] A. Eliasson, J.H.S. Hofmeyr, S. Pedler, B. Hahn-Hagerdal, The xylose
201 reductase/xylytol dehydrogenase/xylylokinase ratio affects product formation in
202 recombinant xylose-utilising *Saccharomyces cerevisiae*, *Enzyme and Microbial.*
203 *Technology* 29 (2001) 288-297.
204
- 205 [6] T.W. Jeffries, Y.S. Jin, Metabolic engineering for improved fermentation of pentoses
206 by yeasts, *Appl. Microbiol. Biotechnol.* 63 (2004) 495-509.
207
- 208 [7] H. Jeppsson, S. Yu, B. Hahn-Hagerdal, Xylulose and glucose fermentation by
209 *Saccharomyces cerevisiae* in chemostat culture, *Appl. Environ. Microbiol.* 62
210 (1996) 1705-1709.
211
- 212 [8] J.M. Jez, T.M. Penning, The ald-keto reductase (AKR) superfamily: an update,
213 *Chem. Biol. Interact.* 130-132 (2001) 499-525.
214
- 215 [9] K.L. Kavanagh, M. Klimacek, B. Nidetzky, D.K. Wilson, The structure of apo and

216 holo forms of xylose reductase, a dimeric aldo-keto reductase from *Candida*
217 *tenuis*, *Biochemistry* 41 (2002) 8785-8795.

218

219 [10] K.L. Kavanagh, M. Klimacek, B. Nidetzky, D.K. Wilson, Structure of xylose
220 reductase bound to NAD⁺ and the basis for single and dual co-substrate specificity
221 in family 2 aldo-keto reductases, *Biochem. J.* 373 (2003) 319-326.

222

223 [11] R.A. Laskowski, M.W. Macarthur, D.S. Moss, J.M. Thornton, Procheck - a Program
224 to Check the Stereochemical Quality of Protein Structures, *Journal of Applied*
225 *Crystallography* 26 (1993) 283-291.

226

227 [12] S. Leitgeb, B. Petschacher, D.K. Wilson, B. Nidetzky, Fine tuning of coenzyme
228 specificity in family 2 aldo-keto reductases revealed by crystal structures of the
229 Lys-274 → Arg mutant of *Candida tenuis* xylose reductase (AKR2B5) bound to
230 NAD⁺ and NADP⁺, *Febs Letters* 579 (2005) 763-767.

231

232 [13] L. Liang, J. Zhang, Z. Lin, Altering coenzyme specificity of *Pichia stipitis* xylose
233 reductase by the semi-rational approach CASTing, *Microb. Cell Fact.* 6 (2007) 36.

234

235 [14] A. Matsushika, H. Inoue, S. Watanabe, T. Kodaki, K. Makino, S. Sawayama,
236 Efficient bioethanol production by a recombinant flocculent *Saccharomyces*
237 *cerevisiae* strain with a genome-integrated NADP⁺-dependent xylitol
238 dehydrogenase gene, *Appl. Environ. Microbiol.* 75 (2009) 3818-3822.

239

- 240 [15] A. Matsushika, S. Watanabe, T. Kodaki, K. Makino, S. Sawayama, Bioethanol
241 production from xylose by recombinant *Saccharomyces cerevisiae* expressing
242 xylose reductase, NADP⁺-dependent xylitol dehydrogenase, and xylulokinase, J.
243 Biosci. Bioeng. 105 (2008) 296-299.
244
- 245 [16] B. Petschacher, B. Nidetzky, Altering the coenzyme preference of xylose reductase
246 to favor utilization of NADH enhances ethanol yield from xylose in a
247 metabolically engineered strain of *Saccharomyces cerevisiae*, Microb. Cell Fact. 7
248 (2008) 9.
249
- 250 [17] M. Rizzi, K. Harwart, P. Erlemann, N.A. Buithanh, H. Dellweg, Purification and
251 Properties of the NAD⁺-Xylitol-Dehydrogenase from the Yeast *Pichia stipitis*,
252 Journal of Fermentation and Bioengineering 67 (1989) 20-24.
253
- 254 [18] C. Verduyn, R. Van Kleef, J. Frank, H. Schreuder, J.P. Van Dijken, W.A. Scheffers,
255 Properties of the NAD(P)H-dependent xylose reductase from the xylose-
256 fermenting yeast *Pichia stipitis*, Biochem. J. 226 (1985) 669-677.
257
- 258 [19] J.F. Wang, D.Q. Wei, Y. Lin, Y.H. Wang, H.L. Du, Y.X. Li, K.C. Chou, Insights
259 from modeling the 3D structure of NAD(P)H-dependent D-xylose reductase of
260 *Pichia stipitis* and its binding interactions with NAD and NADP, Biochem.
261 Biophys. Res. Commun. 359 (2007) 323-329.
262
- 263 [20] S. Watanabe, A. Abu Saleh, S.P. Pack, N. Annaluru, T. Kodaki, K. Makino, Ethanol

264 production from xylose by recombinant *Saccharomyces cerevisiae* expressing
265 protein-engineered NADH-preferring xylose reductase from *Pichia stipitis*,
266 Microbiology 153 (2007) 3044-3054.

267

268 [21] S. Watanabe, T. Kodaki, K. Makino, Complete reversal of coenzyme specificity of
269 xylitol dehydrogenase and increase of thermostability by the introduction of
270 structural zinc, J. Biol. Chem. 280 (2005) 10340-10349.

271

272 [22] S. Watanabe, S.P. Pack, A.A. Saleh, N. Annaluru, T. Kodaki, K. Makino, The
273 positive effect of the decreased NADPH-preferring activity of xylose reductase
274 from *Pichia stipitis* on ethanol production using xylose-fermenting recombinant
275 *Saccharomyces cerevisiae*, Biosci. Biotechnol. Biochem. 71 (2007) 1365-1369.

276

277 [23] S. Watanabe, A.A. Saleh, S.P. Pack, N. Annaluru, T. Kodaki, K. Makino, Ethanol
278 production from xylose by recombinant *Saccharomyces cerevisiae* expressing
279 protein engineered NADP⁺-dependent xylitol dehydrogenase, J. Biotechnol. 130
280 (2007) 316-319.

281

282 [24] D.K. Wilson, K.M. Bohren, K.H. Gabbay, F.A. Quiocho, An unlikely sugar
283 substrate site in the 1.65 Å structure of the human aldose reductase holoenzyme
284 implicated in diabetic complications, Science 257 (1992) 81-84.

285

286 [25] D.K. Wilson, K.L. Kavanagh, M. Klimacek, B. Nidetzky, The xylose reductase
287 (AKR2B5) structure: homology and divergence from other aldo-keto reductases

288 and opportunities for protein engineering, Chem. Biol. Interact. 143-144 (2003)
289 515-521.

Table1
The mutation designs of the PsXR enzyme

Enzyme	Accession No. or mutant	Organism	Coenzyme preference	<u>Amino Acid Sequence</u>					
				2	2	2	2	2	2
				2	2	2	7	7	7
				2	3	4	0	1	2
PsXR	CAA42072	<i>Pichia stipitis</i>	NADPH	V	E	L	K	S	N
AKR1 B7 [§]	P21300	<i>Mus musculus</i>	NADPH [†]	P	D	R	*	*	V
2, 5 DKGRA [*]	AAA83534	<i>Corynebacterium sp.</i>	NADPH [†]	Y	D	*	*	*	V
AR	P15121	<i>Homo sapiens</i>	NADPH [†]	P	D	R	*	*	V
XR	O94735	<i>Pichia guilliermondi</i>	NADPH	*	*	*	*	*	N
XR	Q6Y0Z3	<i>Candida parapsilosis</i>	NADH	L	*	M	*	*	S
XR	O74237	<i>Candida tenuis</i>	NADPH	*	*	M	*	*	L
XR	P87039	<i>Candida tropicalis</i>	NADPH	L	*	*	*	*	N
PsXR	E223A	<i>P. stipitis</i>	This work	*	A	*	*	*	*
PsXR	E223D	<i>P. stipitis</i>	This work	*	D	*	*	*	*
Ps XR	S271A	<i>P. stipitis</i>	This work	*	*	*	*	A	*
Ps XR	AA [‡]	<i>P. stipitis</i>	This work	*	A	*	*	A	*
Ps XR	DA [‡]	<i>P. stipitis</i>	This work	*	D	*	*	A	*

Bold letters represent target mutation sites *The same amino acids as PsXR WT
[‡] Double mutant E223A/S271A (AA) and E223D/S271A (DA)
[†] Strict NADPH dependent enzyme § Aldo-keto reductase family 1, memberB7
^{*} 2,5-Diketo-D-gluconic acid reductase

Table 2

Kinetic parameters of wild-type and xylose reductase mutants for NADPH- and NADH-dependent reactions

Enzymes	Kinetic parameters							
	NADPH				NADH			
	K_m xylose ^a [mM]	K_m ^b [μ M]	k_{cat} ^b [Min ⁻¹]	k_{cat}/K_m [μ M ⁻¹ /min ⁻¹]	K_m xylose ^a [mM]	K_m ^b [μ M]	k_{cat} ^b [min ⁻¹]	k_{cat}/K_m [μ M ⁻¹ /min ⁻¹]
XRWT	97.1 ± 4.8	16.2 ± 1.4	622 ± 22	38.6 ± 2.9	170 ± 23	30.6 ± 1.0	449 ± 22	14.7 ± 1.4
S271A	70.6 ± 8.7	30.1 ± 3.7	874 ± 50	29.0 ± 0.3	180 ± 12	53.3 ± 4.4	480 ± 42	9.00 ± 0.40
E223A	29.8 ± 4.7	35.2 ± 3.7	349 ± 29	9.94 ± 0.44	ND ^d	ND	ND	ND
E223D	114 ± 13	55.4 ± 7.1	314 ± 42	5.65 ± 0.32	376 ± 32	305 ± 11	169 ± 52	0.55 ± 0.15
AA ^c	226 ± 22	17.5 ± 0.7	567 ± 73	32.4 ± 2.7	ND	ND	ND	ND
DA ^c	108 ± 8	20.4 ± 0.4	733 ± 14	36.0 ± 0.3	353 ± 1	391 ± 46	156 ± 29	0.44 ± 0.10

^a Six different concentrations of xylose between 67 and 200 mM were used and NAD(P)H concentration was 150 μ M.^b Six different concentrations of NAD(P)H between 50 and 300 μ M were used and xylose concentration was 400 mM.^c Double mutants E223A/S271A (AA) and E223D/S271A (DA)^d ND: Not detected

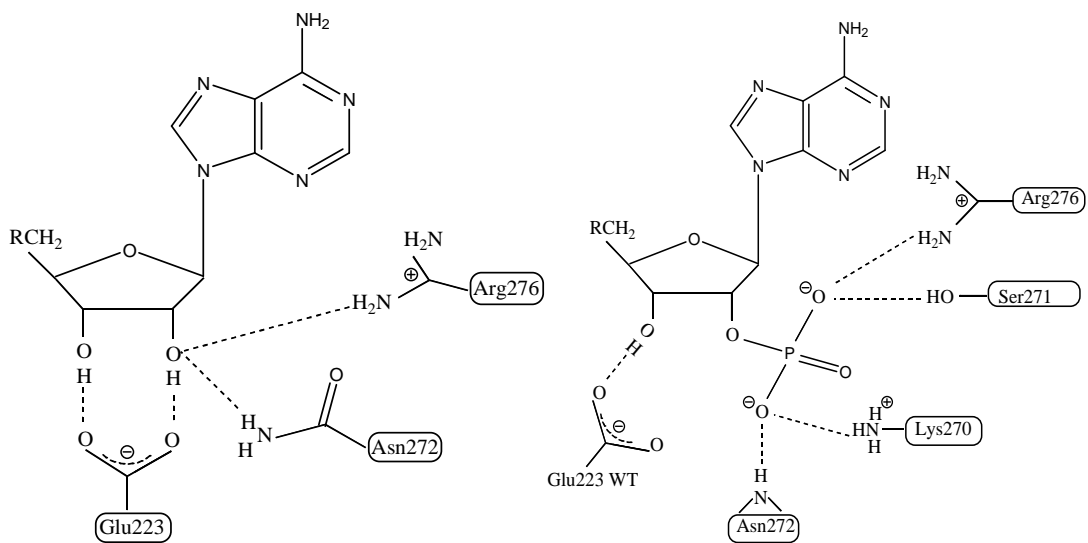


Fig. 1. Schematic diagrams showing the predicted interactions of wild-type PsXR; Left-hand panel: adenosine 2'- and 3'- hydroxy groups in the complex with NAD⁺ and Right-hand panel: adenosine 2'- and 3'- hydroxy groups in the complex with NADP⁺ based on the coenzyme binding sites in CtXR [10].

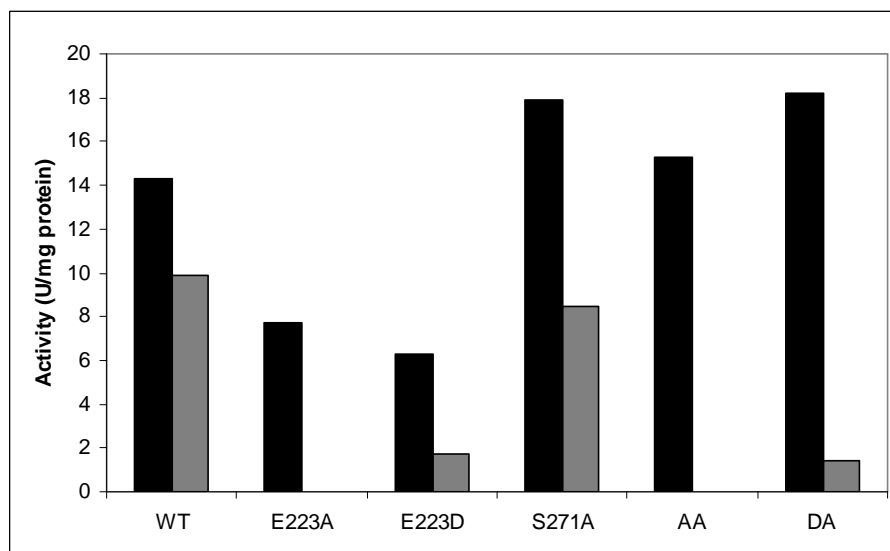


Fig. 2. Enzyme activities of PsXR wild-type and mutated enzymes. Black and grey bars indicated activities with NADPH and NADH respectively; Values are average \pm SD, n=3.